Proc. of the 9th Intl. Conf. of Asian Society for Precision Engg. and Nanotechnology (ASPEN 2022)
15–18 November 2022, Singapore. Edited by Nai Mui Ling Sharon and A. Senthil Kumar
doi://10.3850/978-981-18-6021-8_OR-14-0078

Anisotropy in ultra-precision machinability of additively manufactured Inconel 718 alloys

Yuchao Bai, Yunfa Guo, Hao Wang#

Department of Mechanical Engineering, College of Design and Engineering, National University of Singapore, 9 Engineering Drive 1, Singapore 117575, Singapore

Corresponding Author / Email: mpewhao@nus.edu.sg, TEL: +65 6516 2207

KEYWORDS: Hybrid manufacturing, Ultra-precision machining, Laser powder bed fusion, Microstructure, Cutting force, Machinability

Laser powder bed fusion (LPBF) is highly effective at fabricating metal functional components with complex geometries. However, the poor surface quality of the as-built components necessitates post-machining to meet the high precision requirement. Ultra-precision machining can obtain nanoscale surface roughness through micro-scale material removal, which is a promising process for improving the surface quality of the LPBFed parts. The bottom-up manufacturing method and rapid solidification of the LPBF process result in anisotropy in microstructure and mechanical properties, which will highly affect the machinability of the LPBFed metal parts, especially in ultra-precision machining. At present, this effect is not thoroughly understood. In this study, microstructure and microhardness on the XY and XZ planes of Inconel 718 part fabricated using the LPBF process were characterized first. Then, orthogonal cutting experiments were conducted on the corresponding planes to study the anisotropy in machinability using ultra-precision machining, including cutting force, surface topography and chip morphology. In addition, the effect of cutting speed on the machining process was also investigated systematically. The results show that the LPBFed Inconel 718 alloy has an apparent building-direction-dependent anisotropy in machinability, which corresponds to the microstructure and microhardness. Two distinct microstructural features were observed on the XY and XZ planes, respectively. The side flow on the XZ plane is much severer than that on the XY plane during orthogonal cutting, thereby leading to poor microgroove quality. In addition, the cutting force on the XZ plane is much higher (more than 37.7%) and fluctuates more significantly than that on the XY plane. This study provides an in-depth understanding of the micro-machining of additively manufactured metal parts as well as a reference for improving the surface quality through post-processing.

NOMENCLATURE

LPBF = laser powder bed fusion
CBN= cubic boron nitride
AM=additive manufacturing
SM=subtractive manufacturing

1. Introduction

Metal AM technology is an effective method to fabricate functional components with complex geometric structures, which are difficult or impossible to manufacture by the traditional processes [1]. LPBF, as one kind of metal AM technology, provides greater opportunities for fabricating complex parts due to the ability of high relative density and high manufacturing resolution. However, the LPBFed metal parts are near net shape due to the poor surface finish and low dimension accuracy compared with the SMed counterparts. Therefore, subsequent subtractive, such as post-finishing, on the LPBFed metal parts are usually required for better surface quality. Recently, hybrid additive/subtractive manufacturing is attracting attention from both scientific and industrial fields due to the successful integration of the advantages of AM and SM [2].

However, the anisotropy and microstructural heterogeneity are commonly the features of AMed metal parts due to the bottom-up manufacturing method, which will further influence the machinability, such as cutting force, surface quality and tool wear. Bai et al. [3] analyzed the microstructure and mechanical property of LPBFed maraging steel and found the tensile strength perpendicular to the building direction was the highest. The milling results show that the cutting force and tool wear on the milling side surface (XZ plane) is lower than that in milling the top surface (XY plane) [4]. In addition, Ni et al. [5] reported that the anisotropic mechanical and microstructure were the fundamental reasons for the anisotropic machinability in terms of cutting force and surface roughness. Bai et al. [6] also reported the difference in cutting force and surface quality between XY and XZ planes in micro-cutting LPBFed CuCrZr alloys. Regarding the LPBFed Inconel 718, the anisotropy in mechanical properties induced by microstructure and fibre textures are also reported [7]. Moreover, et al. [8] revealed the relationship between cutting force and anisotropy features in milling LPBFed Inconel 718 alloy. However, the depth of cut in the milling process in this study is very large, which covers several grains in one cutting. Ultra-precision

machining LPBFed Inconel 718 with a depth of cut of several micrometres (much less than the grain size) is not reported.

The present study aimed to investigate the anisotropy in ultra-precision machinability of LPBFed Inconel 718 alloys, in which the effect of single grain will be more significant. First, the microstructural characterization of the XY plane and XZ plane was extracted from the as-built cubic sample. Then, the corresponding microhardness and micromechanical properties were obtained. Finally, micro-grooving cutting experiments were performed on each plane in an ultra-precision machining machine to study the anisotropy in machinability.

2. Experimental procedure

2.1 Sample preparation

The Inconel 718 samples for the machining study were prepared using an LPBF additive manufacturing machine DiMetal-280 via melting Inconel 718 powders layer by layer. The main process parameters are as follows: laser power of 215 W, scanning speed of 900 mm/s, layer thickness of 30 µm and hatching space of 80 µm. In addition, the machine was filled with high-pure argon to prevent oxidation. The powders are spherical and prepared by the water atomization method, which has a particle size range of 15–53 µm. The sample geometry was a 10 × 10 × 10 mm cube.

2.2 Machining experiment

The micro-cutting machining experiments were conducted on a Toshiba ULG-100 ultra-precision machining centre equipped with a Kistler dynamometer for measuring cutting force as shown in Fig. 1. A CBN cutting tool with 0° rake and 10° clearance angles. The cubic samples were fixed onto the air-bearing spindle of the machining centre using a vacuum chuck for successive face turning and micro-groove cutting on the end surface of each sample. Before orthogonal cutting, face turning was performed to get a flat end surface. Then, the dry orthogonal cutting for the micro-grooving test was conducted by holding the sample stationary and feeding the cutting tool along a designated cutting direction. The detailed machining parameters for the face turning and micro-grooving experiments are listed in Table 1. Three grooves for each group of machining parameters were cut to guarantee test repeatability.

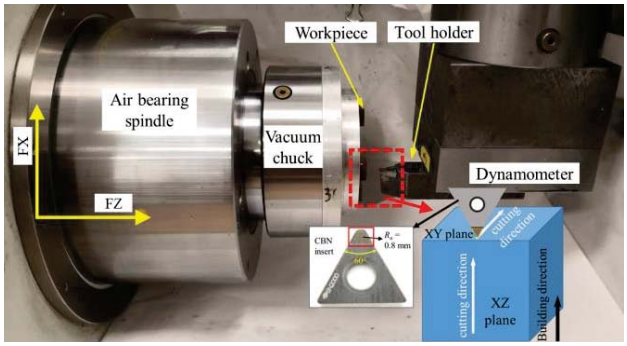

Fig. 1. Setup for ultra-precision machining LPBFed Inconel 718 alloy.

Table 1. The ultra-precision machining parameters for the LPBFed Inconel 718 alloy.

Cutting type	Parameters	Value
Face turning	Spindle speed (rpm)	1,500
	Depth of cut (µm)	3
	Cooling condition	Oil mist
Micro-grooving	Cutting speed (mm/min)	50, 200
	Depth of cut (µm)	5
	Cooling condition	Dry

2.3 Characterization

The microstructural morphology on the XY and XZ plane was observed under a LEXT OLS5000 laser confocal microscope and JEOL JSM-5500LV scanning electron microscope (SEM) after polishing and etching by Copper sulfate hydrochloric acid ethanol solution ($CuSO_4$:HCl:Ethanol = 0.5g:5ml:5ml) for ~40 s and rinsed with alcohol. Microhardness tests were conducted using an Anton Paar MCT3 instrumented indentation tester with a maximum force of 500 mN, loading speed of 500 mN/min, and data acquisition rate of 100 Hz.

3. Results and discussion

3.1 Microstructure

The microstructure of LPBFed Inconel 718 samples is presented in Fig. 2. There are a large number of strip melt tracks on the XY plane, as shown in Fig. 2(a). However, additional arcuate melt tracks are observed on the XZ plane (Fig. 2(d)). In addition, it can be seen from Fig. 2(b, f) that some large columnar epitaxial grains are formed on the XZ plane, which passes through several layers of melt tracks. On the XY plane, there are only some large equiaxed grains. In Fig. 2(c, f), a large number of cellular and columnar sub-structures are observed, which are separated by white boundaries. The space of the sub-structure is between 1 and 2 µm. The formation of this unique sub-structure is due to the high cooling rate during the LPBF process, which causes the presumable aggregation of large atom radii (Nb etc.) to the interdendritic areas [9].

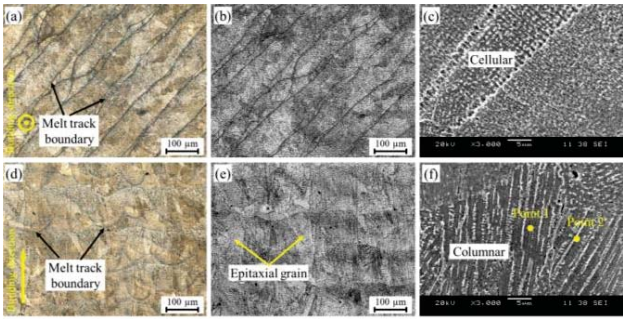

Fig. 2. Optical and SEM microstructure images on (a-c) XY plane and (d-e) XZ plane.

From Fig. 2(f), it is found that the contents (wt %) of Nb element on point 1 (inside the sub-structure) and point 2 (sub-structure

boundary) are 9.13% and 17.83%, respectively, which indicates the aggregation of Nb element to the sub-structure boundary. In addition, it should be noted that the microsegregation will lead to the formation of brittle intermetallic Laves phase. Furthermore, the columnar sub-structures are generally along the building direction, which is caused by the oriented thermal gradient due to the bottom-up manufacturing method. From the above analysis, it can be concluded that there exists anisotropy in microstructure in the LPBFed Inconel 718 alloy, which will also lead to the difference in mechanical properties and machinability between XY and XZ planes.

3.2 Microhardness

To access the anisotropy in mechanical properties, the microhardness and indentation load-depth curves on XY and XZ planes are obtained, as shown in Fig. 3. Ten points were measured on each plane, in which the microhardness of the XZ plane is a little higher than that of the XZ plane. The average microhardness of the former is 353.2 ± 15.2 HV compared to the latter with 326.1 ± 8.3 HV. In addition, there is a large fluctuation in microhardness on the XZ plane, which may be due to the texture [10]. Dynamic mechanical responses of the XY and XZ planes under micron-scale compression are displayed in Fig. 3(b). Under the same maximum load force, the maximum depth of the XZ plane is smaller than that of the XY plane, which implies a higher resistance to deformation of the XZ plane. Furthermore, the elastic part of the indentation work of the XY plane is 11.52%, which is lower than that of the XZ plane (12.33%). This difference indicates that the material recovery of the XY plane is different from that of the XZ plane, which will predictably affect the corresponding cutting forces.

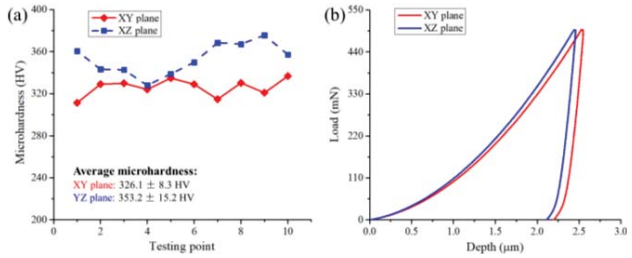

Fig. 3. (a) Microhardness and (b) indentation load-depth curves of XY and XZ planes.

3.3 Machinability

Fig. 4 shows the cutting forces profile curves and average cutting forces of XY and XZ planes under different cutting speeds. It can be observed that the cutting force of the XZ plane is much higher than that of the XY plane. The FX and FZ forces of the XZ plane and XY plane are 6.37 N and 8.94 N, and 3.97 N (reduced by 37.7%) and 5.16 N (reduced by 42.3%), respectively, at a cutting speed of 50 mm/min. With the cutting speed increasing to 200 mm/min, the cutting force decreases slightly for both XZ and XY planes, which may be due to the thermal softening effect. In addition, it should be noted that the cutting force profile curves (FX and FZ) of the XZ plane fluctuate more obviously than that of the XY plane. A similar fluctuation phenomenon is also observed in the corresponding microhardness, which shows a positive correlation between mechanical property and cutting force.

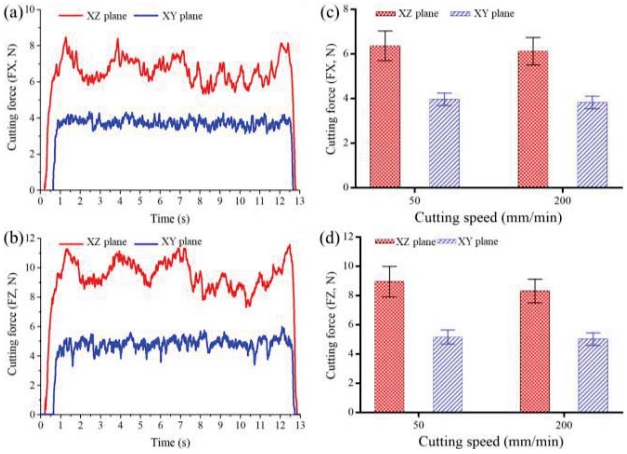

Fig. 4. (a) Cutting force profile curves under cutting speed of 200 mm/min and (b) average cutting forces of XY and XZ planes under cutting speed of 50 mm/min and 200 mm/min. (Depth of cut: 5 μm)

Fig. 5 shows the 3-dimension microgroove morphologies and cross-section line profile on the XY and XZ planes, respectively, under a cutting speed of 200 mm/min and a depth of cut of 5 μm. The most significant difference between them is that there are some large burrs with a height of 0.213–0.682 μm at the edge of the microgroove on the XZ plane. The formation of the burrs is caused by the plastic deformation and side flow of the workpiece material under the effect of a cutting tool [11]. Therefore, the XY plane is much more suitable to fabricate microgroove features due to the better counter quality. In addition, it should be noted that the depth of the microgroove is less than 5 μm, which is caused by material recovery from the contact region between the cutting tool and workpiece after the cutting tool leaves [12].

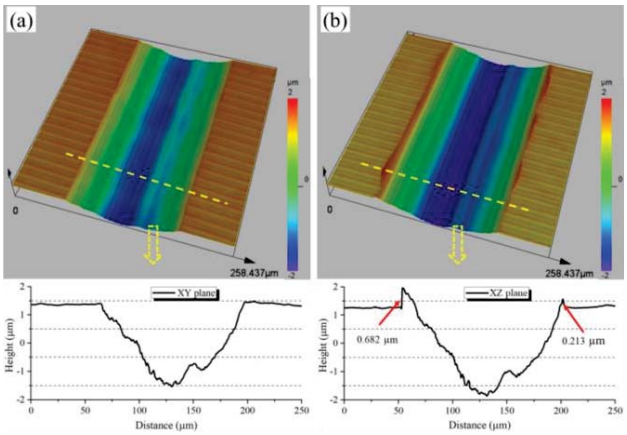

Fig. 5. Microgroove morphologies of (a) XY and (b) XZ planes under cutting speed of 200 mm/min and depth of cut of 5 μm.

From Fig. 6(a, d), it is observwed that the material build-up and fluctuations on the free surface of the chip of the XZ plane are more pronounced. It is well known that the material build-up of the chip will severely hinder the movement of the cutting tool, thereby leading to the increase of cutting force. The material fluctuation of the chips

will cause the fluctuation of cutting force due to the dynamic changes in resistance to the tool from chips, which is consistent with the cutting force profile curves (Fig. 4(a, b)). In addition, there are both large and small serrated morphologies on the chips of the XY and XZ planes, as shown in the high-magnification images. The serrated morphology is formed due to the primary and secondary shear bands during the cutting process. However, the chip serrations of the XY plane are small but many compared to those of the XZ plane, which indicates the different deformation behaviours of the materials in these two chips during the cutting process.

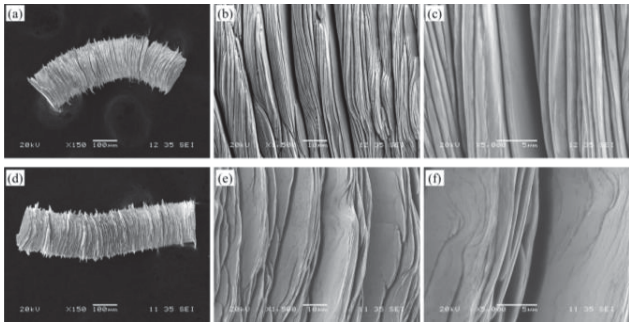

Fig. 6. Chip morphologies of (a-c) XY and (d-f) XZ planes under a cutting speed of 200 mm/min and a depth of cut of 5 μm.

4. Conclusions

This study investigates the machinability of laser powder bed fusion (LPBF) Inconel 718 alloy considering the effect of building direction in ultra-precision machining with a micron-scale depth of cut. The XY plane (perpendicular to the building direction) is characterized by strip melt tracks and micron-scale cellular sub-structures. The XZ plane (parallel to the building direction) has strip-arcuate melt tracks, large columnar epitaxial grains and micro-scale columnar sub-structures. The XZ plane has higher microhardness (353.2HV) and higher elastic part of indentation work (12.33%). The FX and FZ forces of the XZ plane are 6.37 N and 8.94 N, which are reduced by 37.7% (FX) and 42.3% (FZ) when cutting the XY plane. In addition, the cutting force fluctuates sharply when cutting the XZ plane. Increasing the cutting speed will slightly reduce the cutting force. In addition, the surface quality of the microgrooves on the XZ plane is much worse than on the XY plane due to the formation of large burrs.

ACKNOWLEDGEMENT

The authors are grateful for the financial support from the Ministry of Education, Singapore, under its Academic Research Fund (Grant No.: MOE-T2EP50120-0010), and the Agency for Science, Technology and Research, Singapore (Grant No.: A19E1a0097).

REFERENCES

[1] U.M. Dilberoglu, B. Gharehpapagh, U. Yaman, M. Dolen, The Role of Additive Manufacturing in the Era of Industry 4.0, Procedia Manuf. 11 (2017) 545–554. doi:10.1016/j.promfg.2017.07.148.

[2] J.M. Flynn, A. Shokrani, S.T. Newman, V. Dhokia, Hybrid additive and subtractive machine tools - Research and industrial developments, Int. J. Mach. Tools Manuf. 101 (2016) 79–101. doi:10.1016/j.ijmachtools.2015.11.007.

[3] Y. Bai, Y.J. Lee, C. Li, H. Wang, Densification Behavior and Influence of Building Direction on High Anisotropy in Selective Laser Melting of High-Strength 18Ni-Co-Mo-Ti Maraging Steel, Metall. Mater. Trans. A. 51 (2020) 5861–5879. doi:10.1007/s11661-020-05978-9.

[4] Y. Bai, C. Zhao, J. Yang, R. Hong, C. Weng, H. Wang, Microstructure and machinability of selective laser melted high-strength maraging steel with heat treatment, J. Mater. Process. Technol. 288 (2021) 116906. doi:10.1016/j.jmatprotec.2020.116906.

[5] C. Ni, L. Zhu, Z. Zheng, J. Zhang, Y. Yang, J. Yang, Y. Bai, C. Weng, W.F. Lu, H. Wang, Effect of material anisotropy on ultra-precision machining of Ti-6Al-4V alloy fabricated by selective laser melting, J. Alloys Compd. 848 (2020) 156457. doi:10.1016/j.jallcom.2020.156457.

[6] Y. Bai, C. Zhao, Y. Zhang, J. Chen, H. Wang, Additively manufactured CuCrZr alloy: Microstructure, mechanical properties and machinability, Mater. Sci. Eng. A. 819 (2021) 141528. doi:10.1016/j.msea.2021.141528.

[7] M. Ni, C. Chen, X. Wang, P. Wang, R. Li, X. Zhang, K. Zhou, Anisotropic tensile behavior of in situ precipitation strengthened Inconel 718 fabricated by additive manufacturing, Mater. Sci. Eng. A. 701 (2017) 344–351. doi:10.1016/j.msea.2017.06.098.

[8] J.D. Pérez-Ruiz, L.N.L. de Lacalle, G. Urbikain, O. Pereira, S. Martínez, J. Bris, On the relationship between cutting forces and anisotropy features in the milling of LPBF Inconel 718 for near net shape parts, Int. J. Mach. Tools Manuf. 170 (2021). doi:10.1016/j.ijmachtools.2021.103801.

[9] X. Li, J.J. Shi, C.H. Wang, G.H. Cao, A.M. Russell, Z.J. Zhou, C.P. Li, G.F. Chen, Effect of heat treatment on microstructure evolution of Inconel 718 alloy fabricated by selective laser melting, J. Alloys Compd. 764 (2018) 639–649. doi:10.1016/j.jallcom.2018.06.112.

[10] H. Ji, M.K. Gupta, Q. Song, W. Cai, T. Zheng, Y. Zhao, Z. Liu, D.Y. Pimenov, Microstructure and machinability evaluation in micro milling of selective laser melted Inconel 718 alloy, J. Mater. Res. Technol. 14 (2021) 348–362. doi:10.1016/j.jmrt.2021.06.081.

[11] X. Liu, T. Zhou, S. Pang, J. Xie, X. Wang, Burr formation mechanism of ultraprecision cutting for microgrooves on nickel phosphide in consideration of the diamond tool edge radius, Int. J. Adv. Manuf. Technol. 94 (2018) 3929–3935. doi:10.1007/s00170-017-1079-2.

[12] Z. Zhao, S. To, Z. Zhu, T. Yin, A theoretical and experimental investigation of cutting forces and spring back behaviour of Ti6Al4V alloy in ultraprecision machining of microgrooves, Int. J. Mech. Sci. 169 (2020) 105315. doi:10.1016/j.ijmecsci.2019.105315.